SITE-SPECIFIC AND FINE-SCALE WEATHER FORECASTS FOR URBAN AND NON-URBAN AREAS IN THE GREATER CAPITAL REGION, CALIFORNIA

ALTOSTRATUS INC.
Martinez, California
www.altostratus.com

THIS REPORT CONTAINS:

1. EXAMPLE SHORT-TERM FORECAST: September 26 – 28, 2020
2. EXAMPLE LONG-TERM FORECAST: Full year 2050 RCP 8.5 vs. full year 2019

Note: A GIF loop (animation) of the forecast may also accompany this report.

THIS IS AN EXAMPLE FROM A FORECAST OF THE SACRAMENTO REGION.
For questions on methodology, data, models, and validations, or for creating forecasts and weather derivatives specifically for your location, please contact haider@altostratus.com.

1. SHORT-TERM FORECAST EXAMPLE: September 26 – 28, 2020

A cycling 72-hours forecast initiated at 0600 UTC, September 26, 2020 is presented here. The first 24 hours are discarded as spin-up period. A short-term forecast of any length (e.g., up to 10 days out) can be carried and a report prepared upon request. To provide an example, this summary shows results from 0000 PDT, September 27 through 2300 PDT, September 28 (local time in California) and, to limit length, only a few sample hours and locations are discussed. Upon request, reports will be fully detailed and accompanied with animations, as well.

Figure 1.A depicts the forecast temperature field at 1600 PDT, September 27 in the greater Capital region (Sacramento Valley and surrounding areas)[1]. The temperature range in this domain at this hour is 15 to 39 °C (59 – 102 °F) displayed at 1-°C intervals. The cooler parts are found in the NE (Lake Tahoe area) and the warmer parts are in the central and northern areas.

Figure 1.B shows the temperature field at 2000 PDT, September 27, when non-urban areas start to cool down faster than urban parts (heat island effect). At this hour, the temperature range is 11 to 32 °C (52 – 90 °F) displayed at 0.9-°C intervals. The urban areas can be as much as 4 °C (7.2 °F) warmer than their surroundings. The warmest parts at this hour are in the northern half of Sacramento County, around downtown Sacramento, and in the AB617 communities. Other urban areas that are warmer than their surrounds include Yuba City / Marysville, Woodland, Davis, El Dorado Hills, Placerville, Galt, and Fairfield, among others.

Figure 1.C is a screen grab from animation showing the temperature and wind fields at 1900 PDT, September 27, 2020. The urban heat island effect is very conspicuous. Figure 1.D is the forecast temperature field at 1600 PDT, September 28, the day with the highest temperatures of this episode. In this case, the range is 20 to 39 °C (68 – 102 °F) shown at 0.8-°C intervals. At this

[1] The small fine black lines outline the AB-617 communities defined by the Sacramento Metropolitan AQMD.

hour, some urban areas stretching from Elk Grove to Folsom (mostly south of the American River) are actually slightly cooler than the surrounding regions, whereas the areas from downtown Sacramento to Roseville and Lincoln (north of the American River) are warmer.

Figure 1: Forecast air temperature in the greater Capital region.

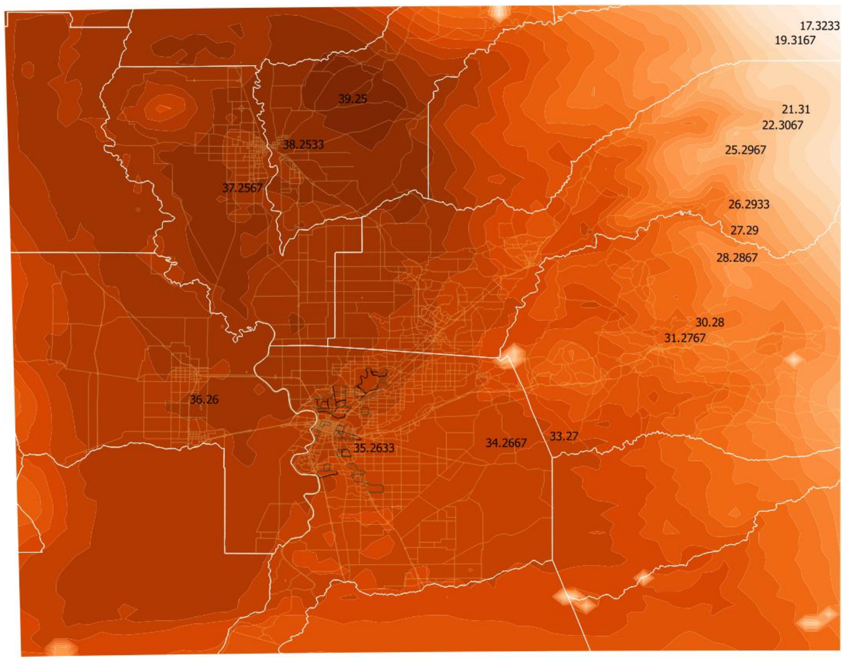

1.A: 1600 PDT September 27, 2020: 15 to 39 °C (59 – 102 °F) by 1-°C intervals

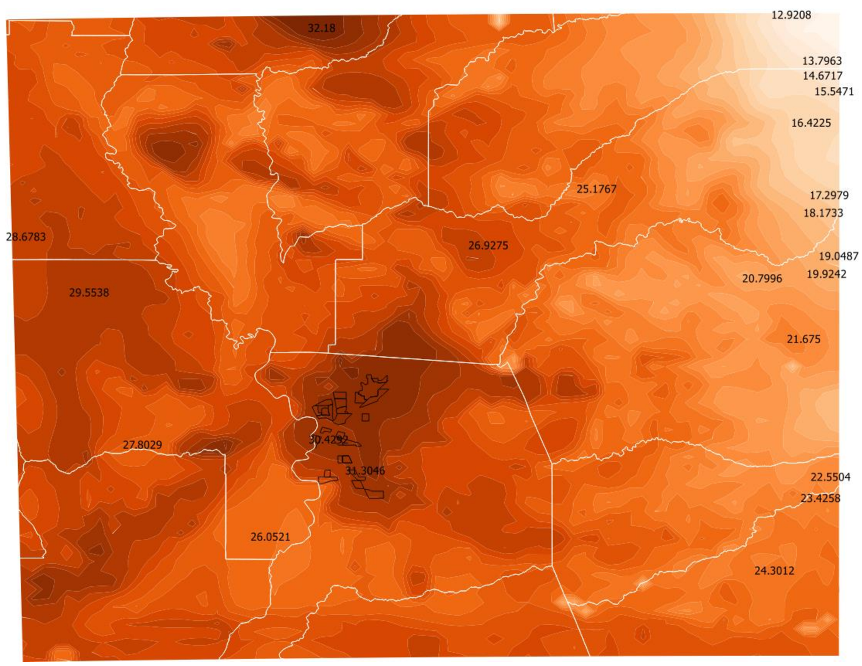

1.B: 2000 PDT September 27, 2020: 11 to 32 °C (52 – 90 °F) by 0.9-°C intervals

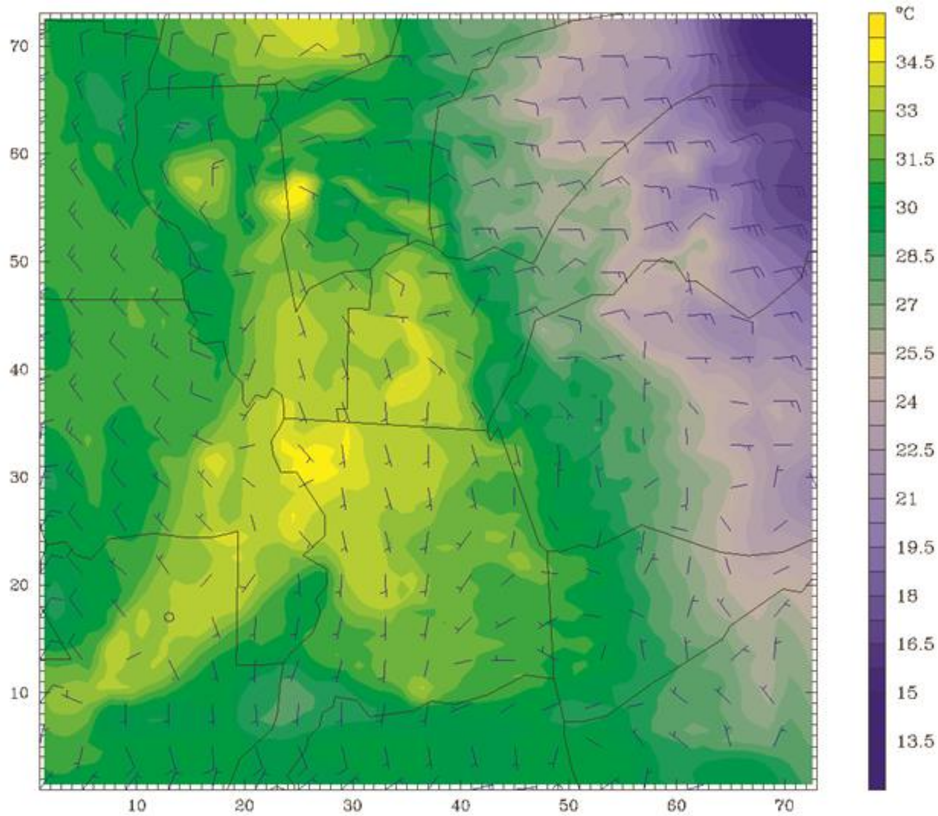

1.C: Screen grab from animation showing temperature (°C) and wind-vector field (m s^{-1}; full barb = 5 m s^{-1}) at 1900 PDT 9/27/2020, an hour when the wind, atypically for this episode, shifts to southerly in the central domain and northwesterly in the western domain (also see Figure 3, circled number 9)

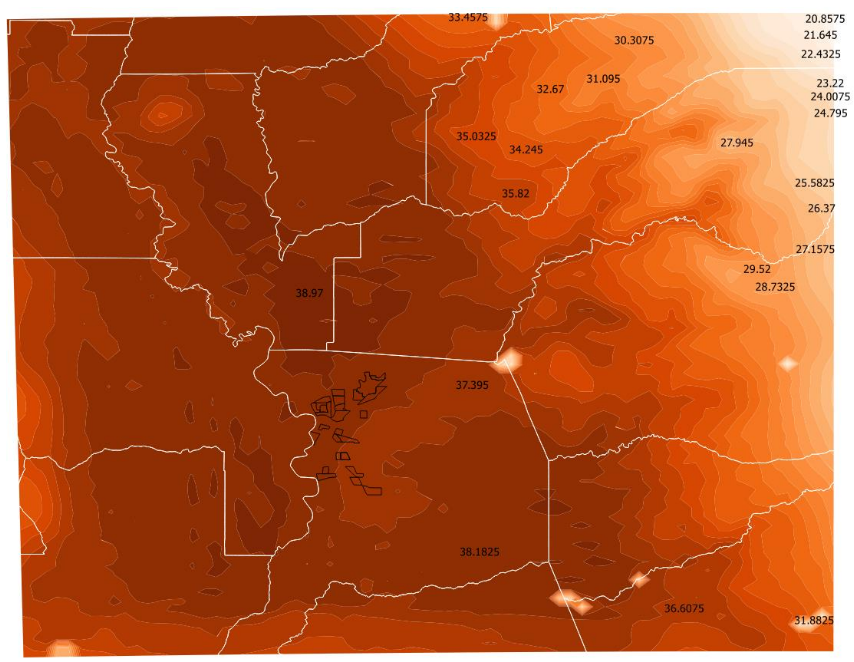

1.D: 1600 PDT September 28, 2020: 20 to 39 °C (68 – 102 °F) by 0.8-°C intervals

The forecasts are carried out daily, typically for 3 to 10 days out (discarding the first day as spin-up period), and in a cycling fashion, meaning, a moving 3 to 10 days-period initialized every 12 hours (or any other time interval desired by the data user). The modeling is site specific and carried out at fine resolutions (1 km to 100 m, depending on area) and results can be provided in detail for any desired location in the domain shown in Figure 2, as an example.

Random urban and non-urban locations (white circles) at 34 points shown in Figure 2B have been selected for extraction of location-specific point forecasts, as examples in this report. In the following discussion, three such locations are presented: (1) a location in downtown Sacramento, (2) a location in North Highlands, and (3) a location in Woodland (the three black circles in Figure 2B).

For each of these three sample locations, weather variables and derivatives are presented in Figure 3. To provide a quick reference, circled numbers are added to each graph, corresponding to the following variables:

- ❶ Air temperature (°C) at 2 m AGL or 2 m above roof level in urban areas (read on left scale);
- ❷ Dew point temperature (°C) (read on left scale);
- ❸ Relative humidity (%) read on right scale;
- ❹ Shortwave radiation at surface (W m^{-2});
- ❺ Longwave radiation at surface (W m^{-2});
- ❻ Air-temperature difference (°C) relative to Sacramento Executive AP (read on right scale);
- ❼ Wind speed (m s^{-1}) at 10 m AGL (read on left scale);
- ❽ Heat Index (NWS), in °F; and
- ❾ Wind direction (°), read on left scale.

The forecast shows air temperatures peaking at around 38 °C (°100 F) at 1600 PDT on September 28 at these three locations (circled number 1 in Figs. 3.1, 3.8, 3.15) and, at the same time, relative humidity (circled number 3) reaching low values of 8 – 10%, hence the higher fire danger in the area, especially when coupled with high winds (see circled number 7 in Figs. 3.3, 3.10, 3.17). The calculated NWS Heat Index (circled number 8 in Figs. 3.4, 3.11, 3.18) shows exceedances above the “Extreme Caution” level at these locations, especially from 1300 to 1800 PDT on September 28th, which is further exacerbated by high incoming solar radiation (circled number 4 in Figs. 3.2, 3.9, 3.16) from the cloudless skies (i.e., un-attenuated solar radiation profiles).

Relative to Sacramento Executive Airport (SAC), which is a standard local monitor used in reporting weather conditions in this region, downtown Sacramento can be cooler or warmer and, in this particular 2-day interval, it is warmer by up to 1.25 °C (2.3 °F) during the day and by as much as 2.5 °C (4.5 °F) at night (circled number 6). North Highlands has a similar pattern, roughly, but can be as much as 4 °C (7.2 °F) warmer than SAC during the day. On the other hand, Woodland is warmer than SAC at all times, particularly during the day. These differences are shown with the circled number 6 in Figs. 3.3, 3.10, 3.17.

For each of these three locations, wind direction (circled number 9) is also potted against wind speed (circled number 7 in Figs 3.5, 3.12, 3.19). As can be seen, wind approach during these two days is consistently from NNW to NNE (between 330° and 10°), regardless of where the air mass originated from, except for the last few hours on September 28, when it switches to roughly southerly flow. Because the air masses are originating mostly over areas to the north or northeast (also air-mass trajectory Figs. 3.6, 3.13, 3.20), the air is drier and warmer than if it were coming from the south or southwest (e.g., the SFBA sea breeze), which further contributes to fire danger. The last graph for each location is a sample cumulative metric of degree-hours, DH (°F·hr), calculated as a total for the period September 27 – 28, 2020. The DH is given relative to four random, but commonly-used thresholds (65, 78, 90, and 95 °F) as shown in Figs. 3.7, 3.14, and 3.21.

Figure 2: Geographical areas and locations of sample forecast points.

(Sacramento Executive Airport (SAC) is the southern of the two red-circled white points)

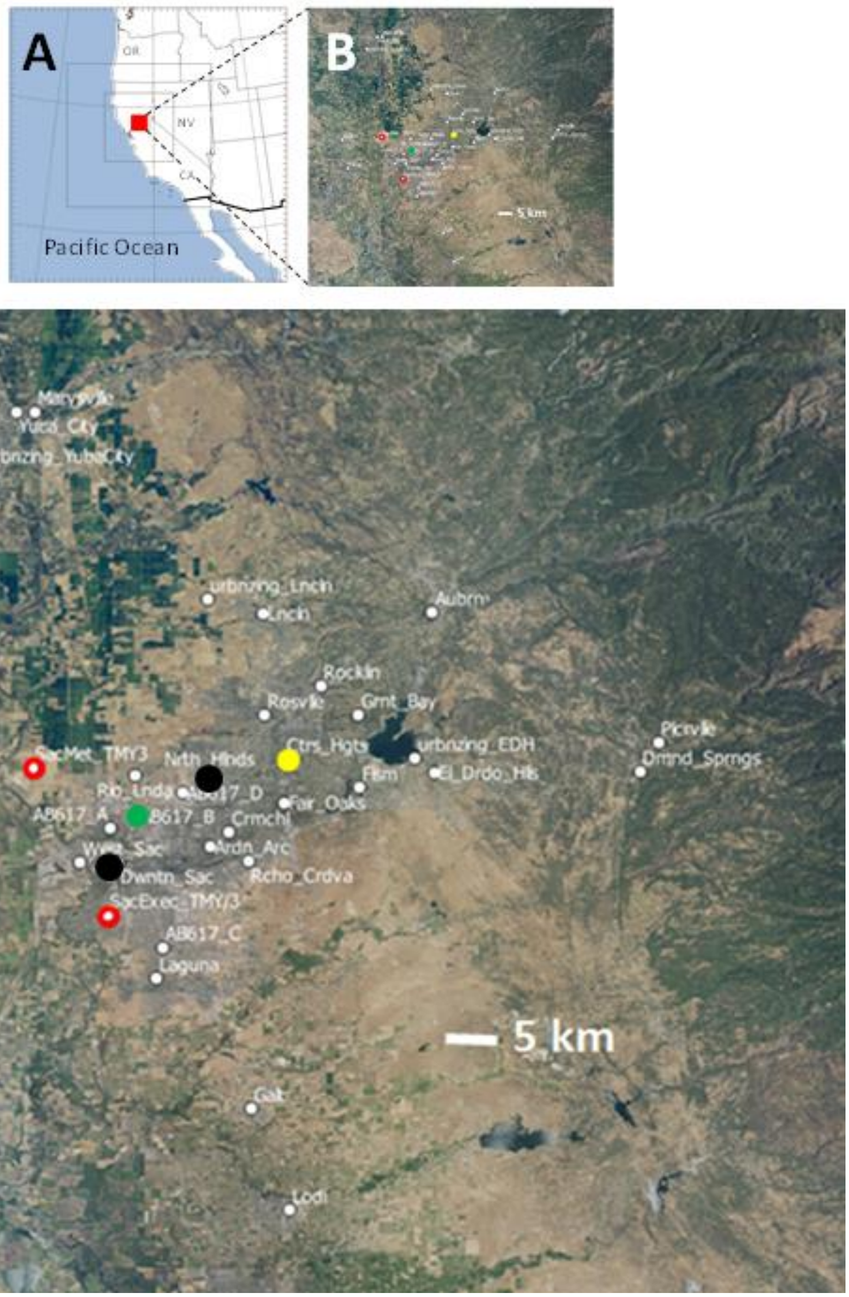

Figure 3: Sample location-specific hourly weather-forecast variables.

(see page 4 for the definition of circled numbers)

Downtown Sacramento

Forecast: September 27 – 28, 2020

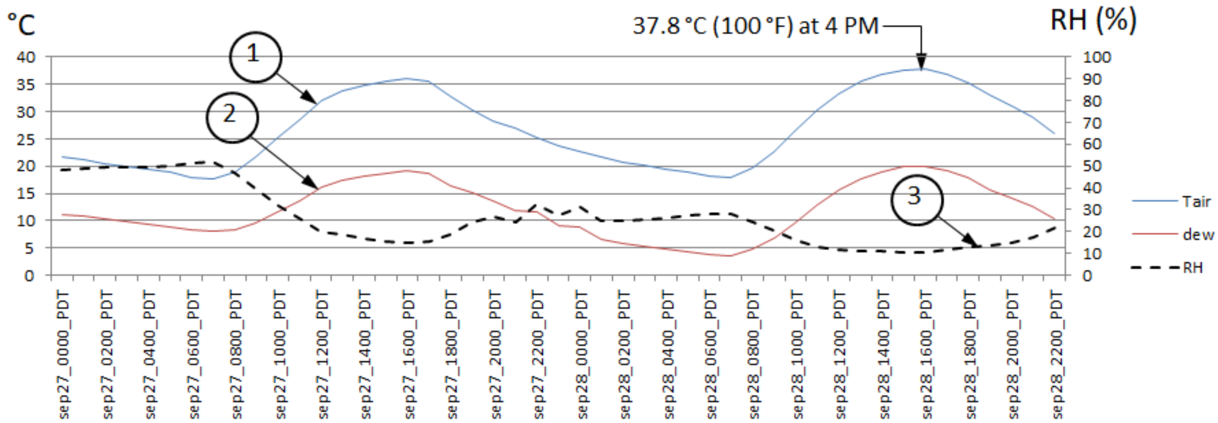

3.1 Air temperature, Dew point, and Relative humidity (Downtown)

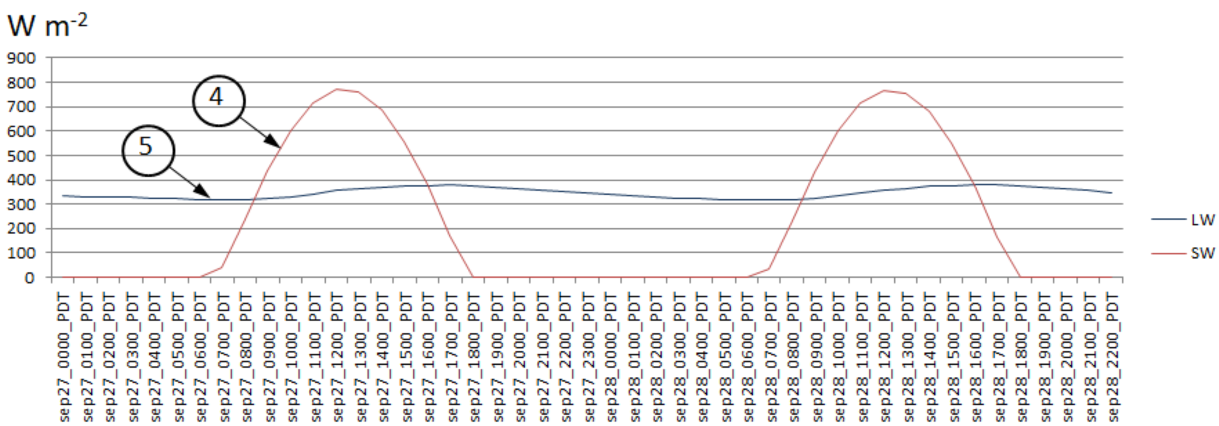

3.2 Short- and long-wave radiation at surface (Downtown)

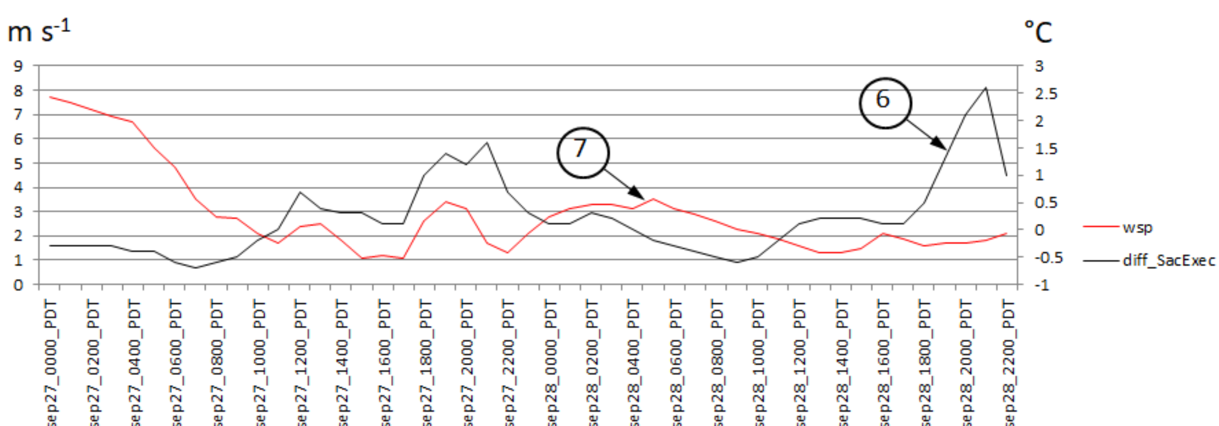

3.3 Wind speed and Temperature departure from SAC (Downtown)

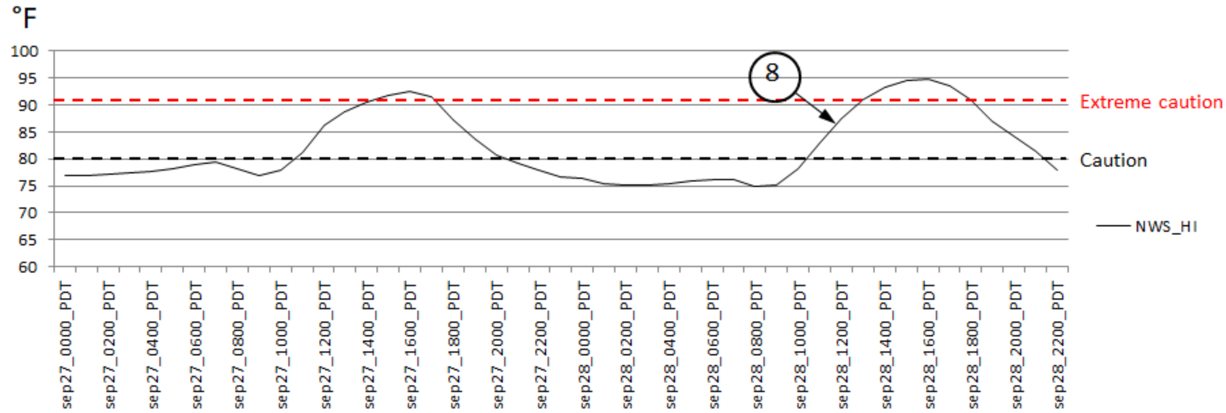

3.4 Heat index (NWS HI) (Downtown)

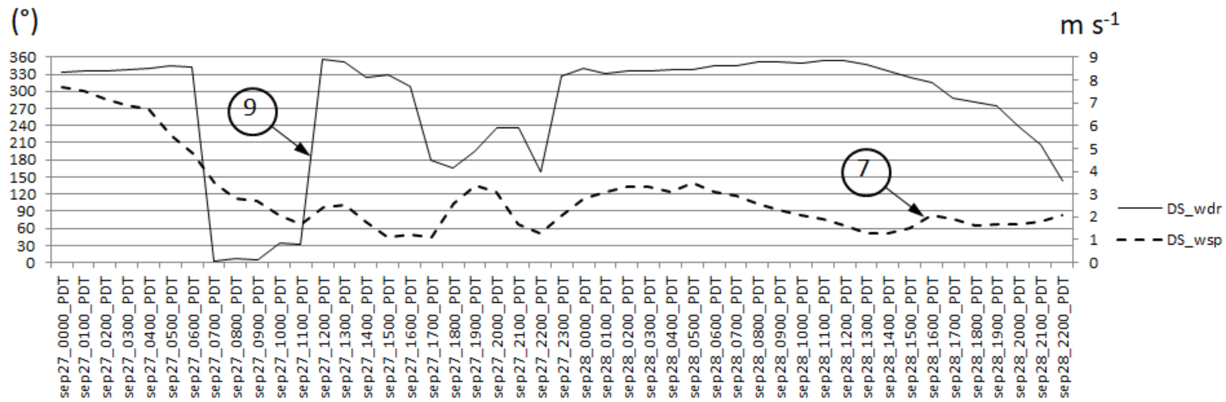

3.5 Wind direction and Wind speed (Downtown)

3.6 Air mass arriving downtown Sacramento at 1400 PDT 9/27 (orange) and 1400 PDT 9/28 (white). Dots spacing is 10 minutes.

- Rain probability = 0%
- Snow probability = 0%

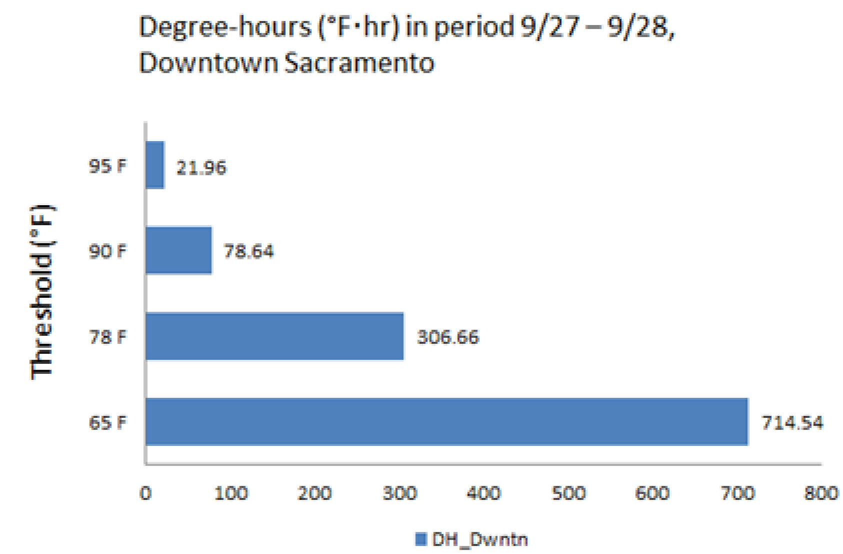

3.7 Degree-hours above given thresholds (Downtown)

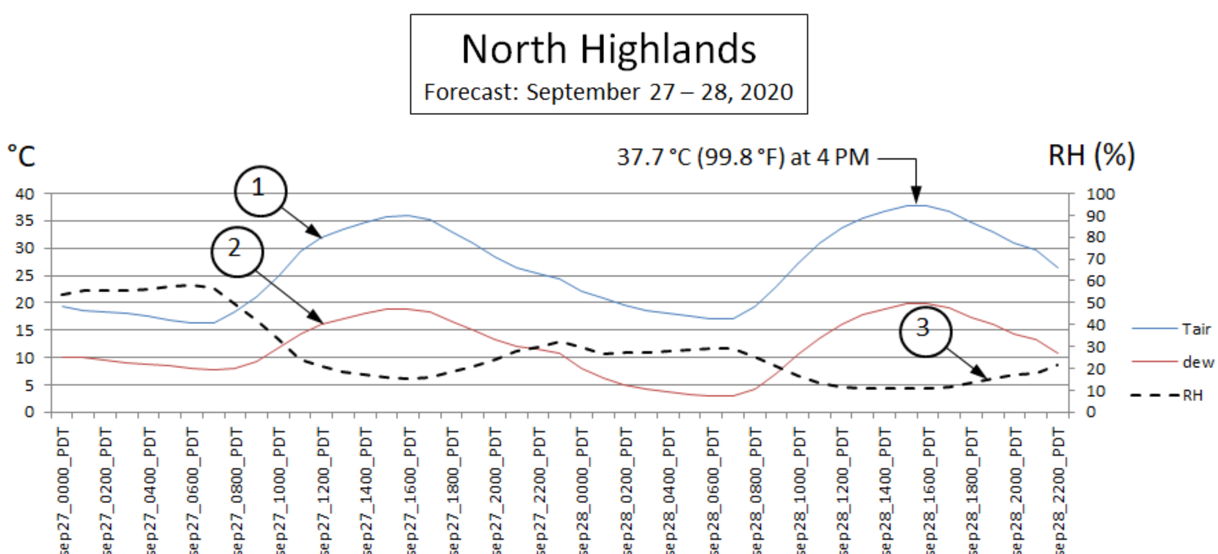

3.8 Air temperature, Dew point, and Relative humidity (North Highlands)

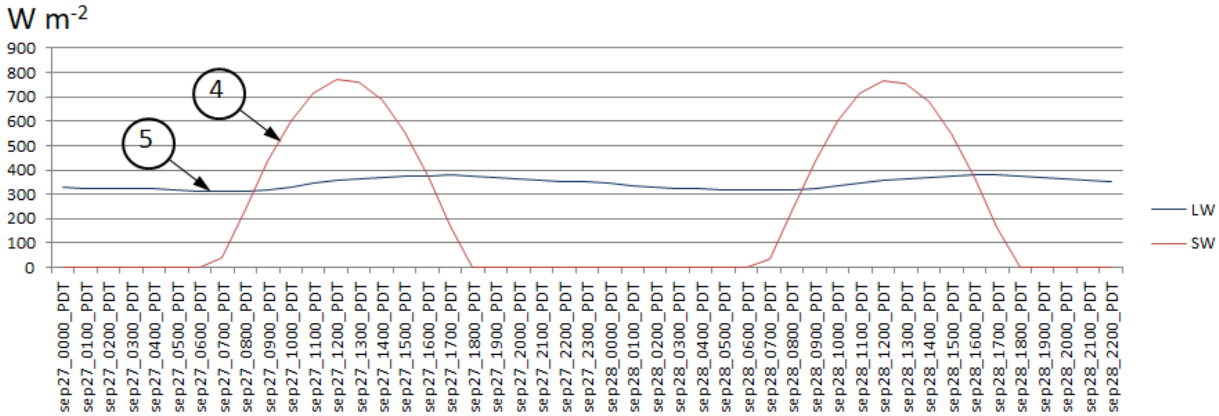

3.9 Short- and long-wave radiation at surface (North Highlands)

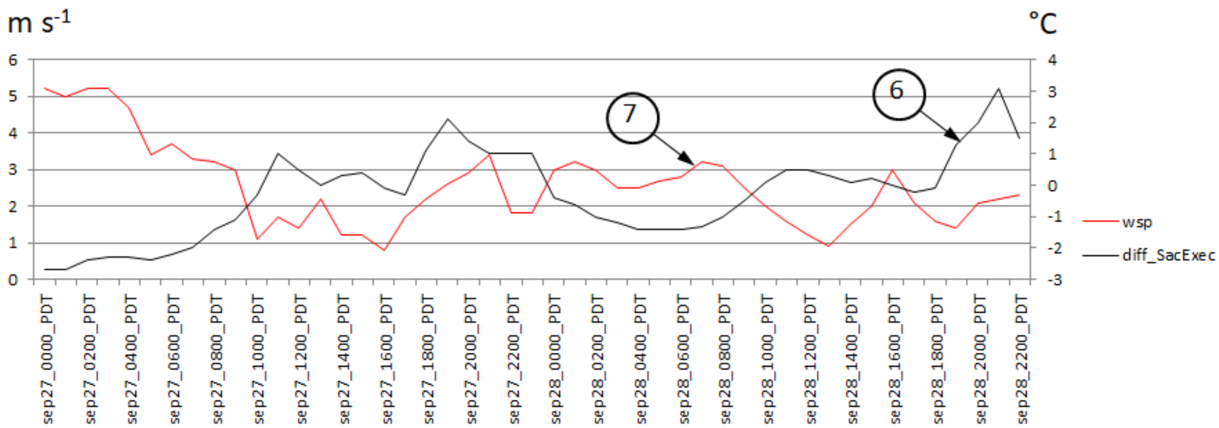

3.10 Wind speed and Temperature departure from SAC (North Highlands)

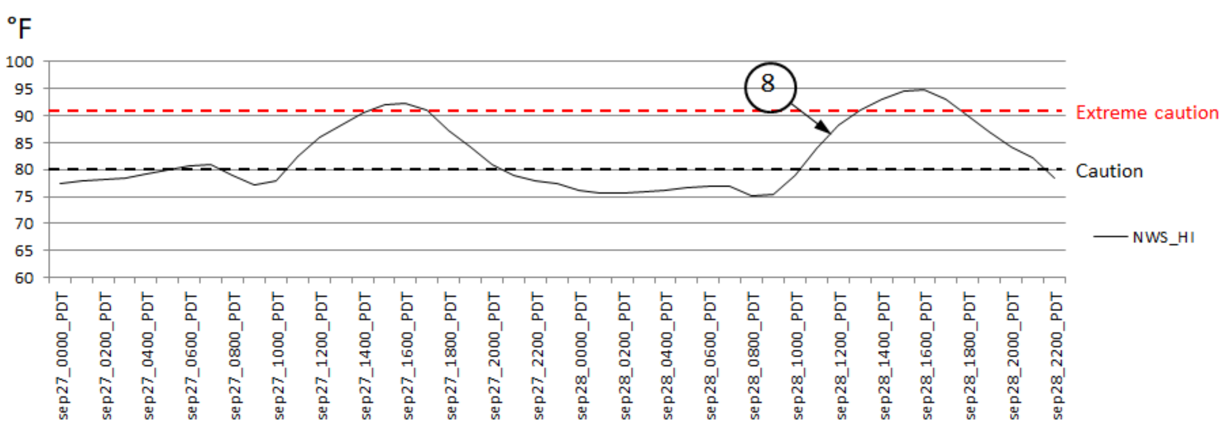

3.11 Heat index (NWS HI) (North Highlands)

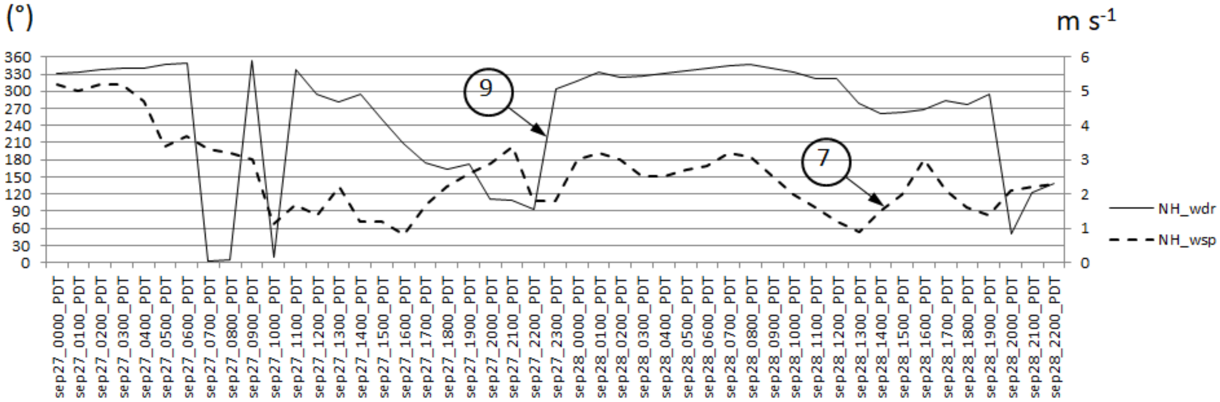

3.12 Wind direction and Wind speed (North Highlands)

3.13 Air mass arriving North Highlands at 1400 PDT 9/27 (orange) and 1400 PDT 9/28 (white). Dots spacing is 10 minutes.

- Rain probability = 0%
- Snow probability = 0%

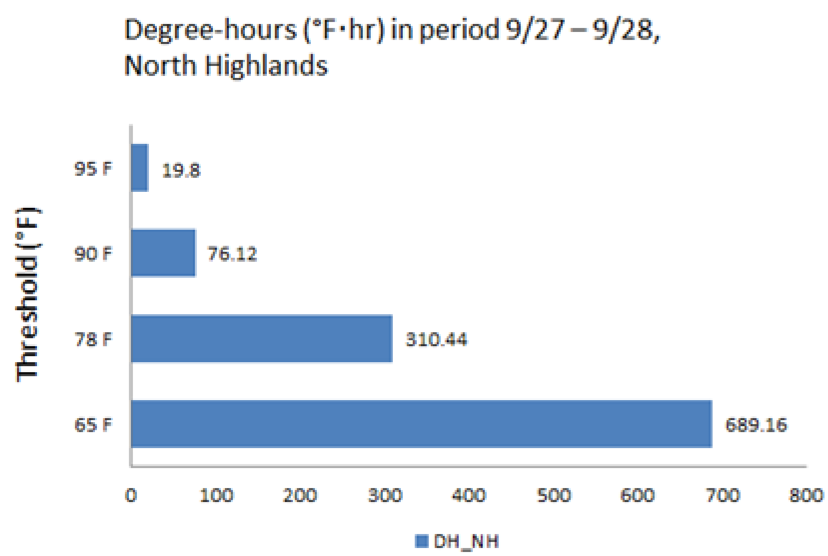

3.14 Degree-hours above given thresholds (North Highlands)

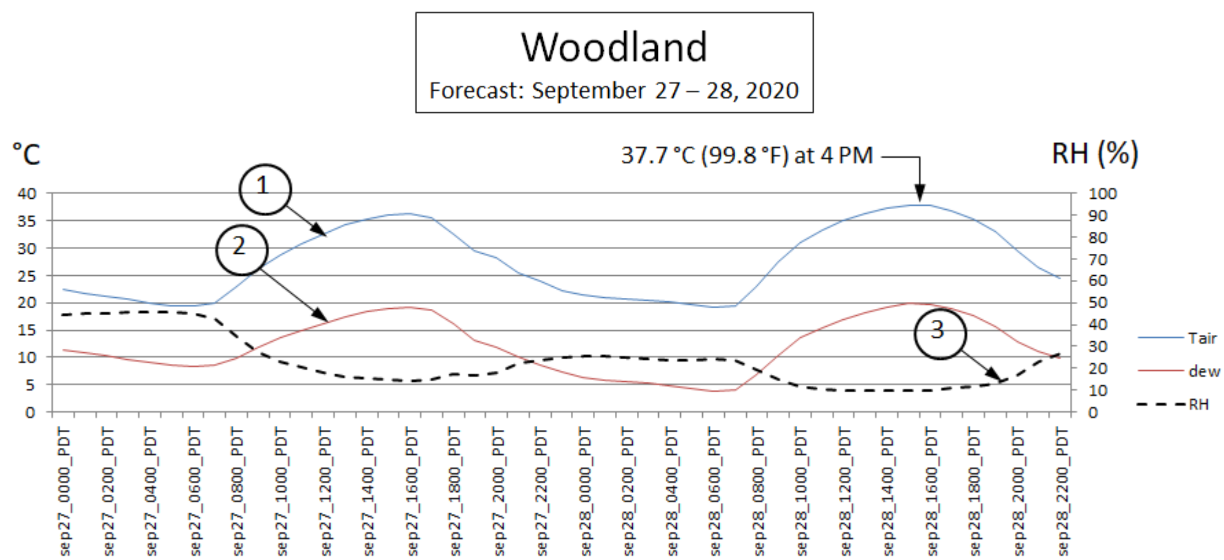

3.15 Air temperature, Dew point, and Relative humidity (Woodland)

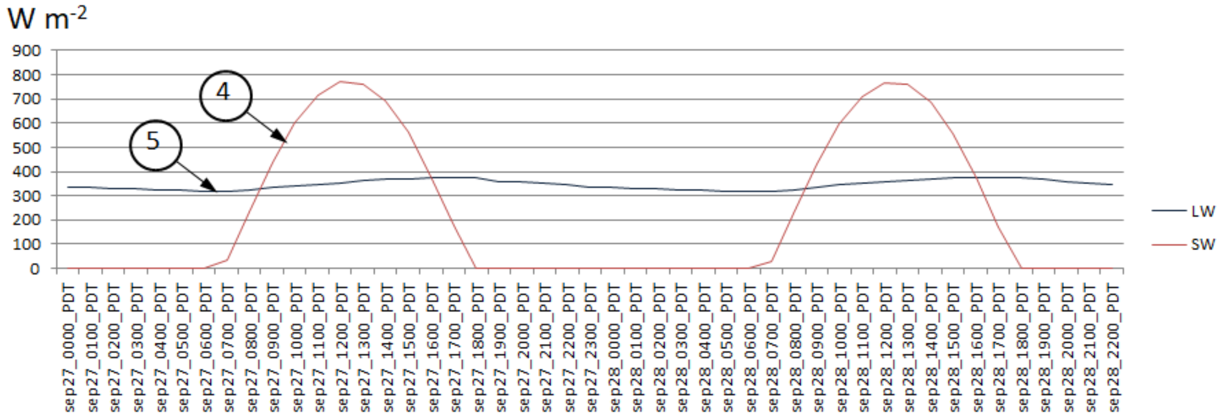

3.16 Short- and long-wave radiation at surface (Woodland)

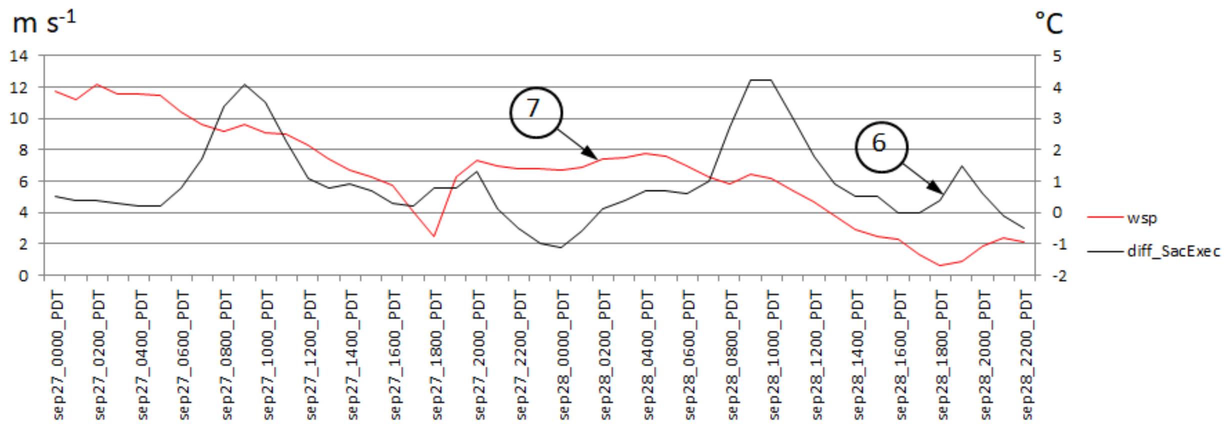

3.17 Wind speed and Temperature departure from SAC (Woodland)

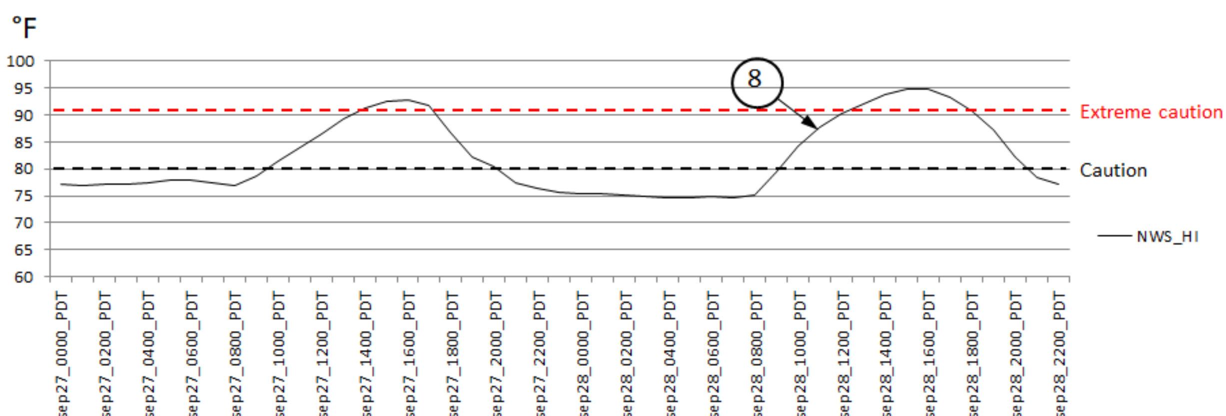

3.18 Heat index (NWS HI) (Woodland)

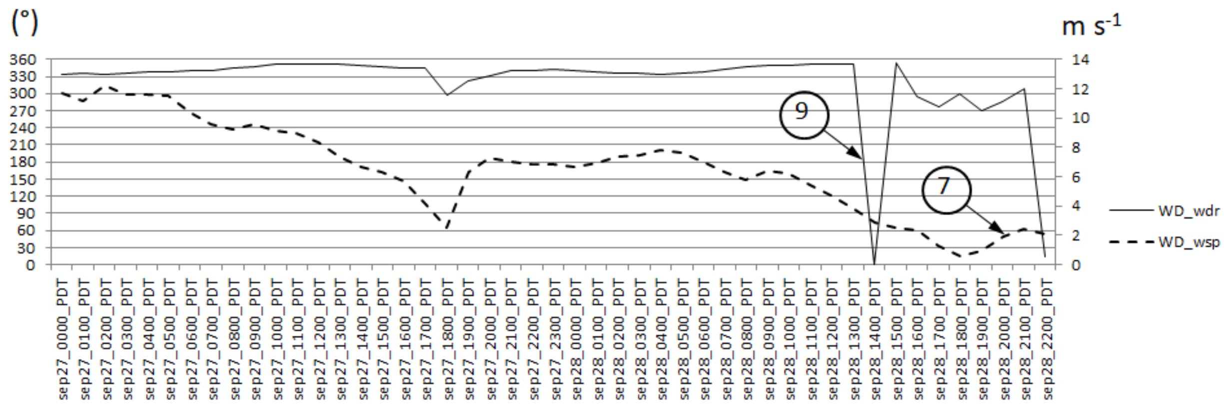

3.19 Wind direction and Wind speed (Woodland)

3.20 Air mass arriving Woodland at 1400 PDT 9/27 (orange) and 1400 PDT 9/28 (white). Dots spacing is 10 minutes.

- Rain probability = 0%
- Snow probability = 0%

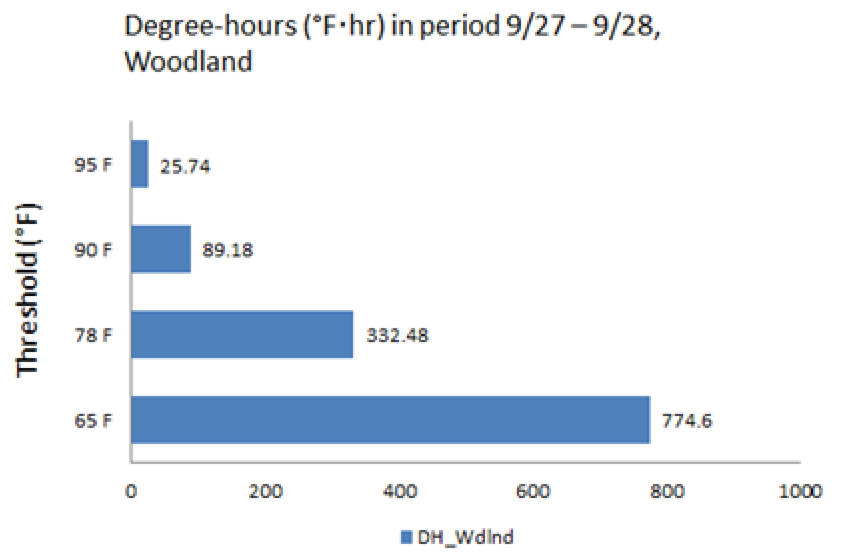

3.21 Degree-hours above given thresholds (Woodland)

A brief overview of other random sample locations (Figure 4) relative to SAC reveals that AB-617 community "A" is general cooler at night but warmer during the day compared to SAC, whereas community "C" is generally similar to SAC. Auburn is warmer at night than SAC but otherwise roughly similar during the day. Citrus Heights is slightly cooler than SAC at night and slightly warmer during the day. Davis is warmer than SAC at all times during these two days and can be up to 4 °C (7.2 °F) warmer in the daytime during this episode.

Diamond Springs is up to 3.8 °C warmer during the night and up to 3.5 °C (6.3 °F) cooler than SAC during the day, while Folsom is generally similar to SAC. Lincoln is cooler at night and warmer during the day. Marysville is warmer than SAC during the day but can be cooler or warmer during the night and early morning hours. Rocklin is relatively similar to SAC during the day but can be warmer or cooler at night. Sacramento Metropolitan Airport is cooler than SAC at night, but warmer during the day by as much as 3.8 °C (6.8 °F). This is significant since these two airports are often used interchangeably as sources of weather files and data for energy forecasting, analysis, and modeling of this region, and this shows that they can be quite different in terms of microclimates. West Sacramento is slightly cooler during the night and slightly warmer than SAC during the day (2 °C, or 3.6 °F). Finally, in Yuba City, it is warmer during the day (up to 2 °C) but, at night, it can be cooler (up to 2 °C or 3.6 °F) or warmer (up to 4 °C, 7.2 °F) than SAC.

Figure 4: Hourly temperature at sample locations (vertical axis) versus Sacramento Executive Airport (horizontal axis) for September 27 – 28.
(the red line is the identity line)

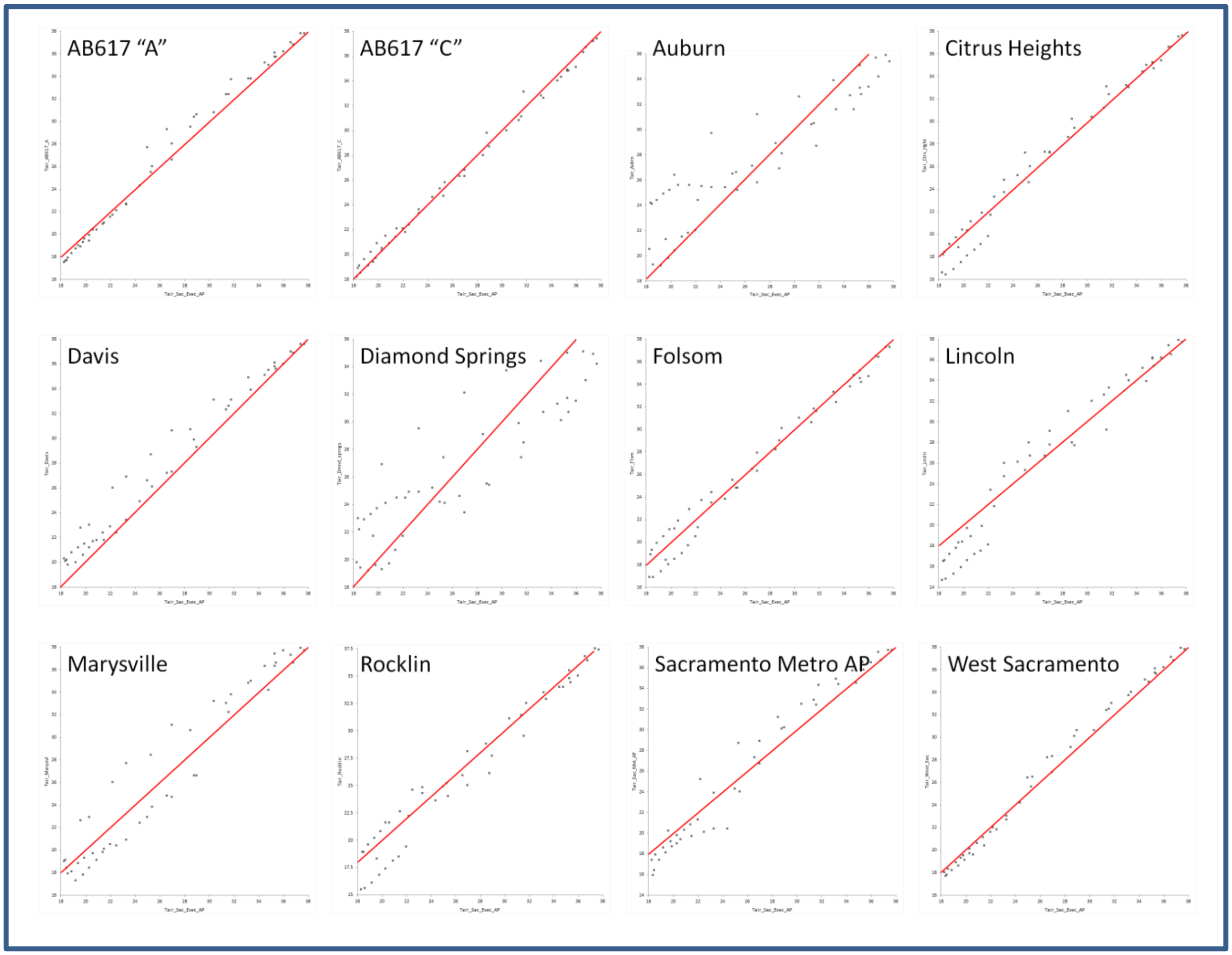

2. EXAMPLE LONG-TERM FORECAST: Full year 2019 to full year 2050 RCP 8.5

In the following discussion, two random urban locations are compared to Sacramento Executive Airport (SAC) which is the source of Typical Meteorological Year data (TMY/TMY3) used in energy modeling and calculations for the region. The two locations are:

1. An AB-617 community “B”, one of ten disadvantaged areas identified by the Sacramento Metropolitan Air Quality Management District (SMAQMD). This is referred to as “AB” in the following discussion and is 12 km NNE of SAC. It is identified with a green circle in Figure 2B.
2. A location in the City of Citrus Heights, referred to as “CTRS” in this discussion, and is 25 km NE of SAC. It is identified with a yellow circle in Figure 2B.

The comparisons among these three locations can be done following one or more approaches, including the following:

Approach 1: Atmospheric-model perturbations (uWRF) applied to current TMY/TMY3 weather fields at SAC via departures from monthly means (indirect mapping) or hour-to-hour departures (direct mapping). This results in *synthetic* weather data, meaning that they are modifications to current TMY data. Conceptually, for a variable V, this can be described as:

$$V_{TMY} = \overline{V}_{TMY} + V'_{TMY} \ ; \quad V_{uWRF} = \overline{V}_{uWRF} + V'_{uWRF} \ ; \quad \boldsymbol{and}: \quad V_C = \overline{V}_{TMY} + V'_{uWRF}$$

where V_c is the desired computed value of the variable (the equations are generic, i.e., they can be applied in space or in time, as well as both simultaneously);

Approach 2: Model perturbations applied to observational data from metar and other high-quality weather stations, e.g., from NOAA. This no longer produces a *synthetic* weather file as compared to approach 1 and is more realistic because the observations come not from a composite weather datasets (e.g., TMY) but, rather, from dynamically-consistent hourly and sub-hourly observations for a specific time interval, e.g., a full year. Thus, in concept, this is similar to the 8-hour ozone relative reduction factor (RRF) used by air-quality management and control agencies, but applied here to meteorological variables; and

Approach 3: Absolute model fields (whether deterministic or probabilistic) at any and all locations of interest for the desired periods. In this case, the fields are absolute, dynamically consistent, and no longer based on departures from some spatial or temporal means, such as from existing weather files.

In all approaches, variables of interest include air temperature, dew-point, relative humidity, short- and long-wave radiation, diffuse radiation, wind speed, wind direction, rainfall, and snow. Some of these are discussed further below and shown in Figures 5 – 7.

Thus, approach 3 is the most correct, scientifically-sound approach, and the one recommended for use. However, all three options can be made available to interested parties if so desired. Although rarely the case, approach 1 can result in unrealistic values at times. For instance, in the sample data discussed below, this approach can produce temperatures in 2050 RCP 8.5 that reach 50 °C during a few hours in the year (outliers). In the datasets discussed below, examples from approaches 1 and 3 are provided.

In this discussion, locations SAC, AB, and CTRS are compared. As space is limited in this short example report, only air temperature comparisons are shown in somewhat larger graphics in Figure 5 and summarized with additional information in Figure 6. For other variables, postage-stamp graphs are shown in Figure 7 to provide a more qualitative and general assessment. In all graphs, the red ellipses represent the bivariate normal density, provided here merely as a visual aid to discern outliers or extreme values in the data from 8760 hours, in respective years, and the red line is the identity line.

In general, the graphs in Figures 5 and 7 can be grouped into two sets: (1) those representing spatial comparisons, i.e., comparing variables at different locations but for the same timestamps and (2) those representing temporal comparisons at different timestamps (e.g., across different years) but at the same respective locations. Thus one observation that can be made is that the spatial comparisons (graphs A1, A2, D1, and D2 in Figure 5 and rows R1, R2, R7, and R8 in Figure 7) have a smaller scatter than the temporal comparisons. This is expected since the spatial variations during a given timestamp over relatively short distances are likely to be smaller than comparing, say, a certain hour in current and future climates.

Graphs A1 and A2 (in Figure 5) are from approach 1 (for current climate, 2019) and show dry-bulb temperature increasing away from SAC location because of intra-urban heat transport as well as the synoptic northerly flow during these days. Because of this process, AB has a net increase of 5190 °C·hr yr^{-1} relative to SAC, whereas CTRS has a net increase of 8157 °C·hr yr^{-1} relative to SAC (non-threshold). The annual all-hours temperature averages at SAC, AB, and CTRS are 15.55, 16.14, and 16.48 °C (Figure 6). Thus, over a relatively short distance between these stations (Figure 2B), an annual-average 1 °C difference can result because of intra-urban microclimate effects, which is very significant. The largest increases in temperature relative to SAC occur during the mid-ranges of absolute temperature and can be as much 4 °C warmer in AB and up to 6 °C (10.8 °F) warmer in CTRS at any given hour within that temperature range. This can also be seen in graphs A1 and A2 (entasis) as well as in the upward shift of the interquartile ranges seen in Figure 6, differences A1 and A2, where the 1st quartile is relatively unchanged but the 3rd quartile is higher.

Graphs B1, B2, and B3 (in Figure 5) are spatial comparisons based on approach 1, but for the year 2050 (RCP 8.5). Thus, B1 is SAC in 2050 relative to TMY3, B2 is AB in 2050 vs. AB in 2019, and B3 is CTRS in 2050 relative to CTRS in 2019. The net warming (from 2019 to 2050) at SAC is 8649 °C·hr yr^{-1} (or 0.99 °C·hr hr^{-1}), at AB the net warming is 9187 °C·hr yr^{-1} (or 1.05 °C·hr hr^{-1}), and at CTRS, it is 10321 °C·hr yr^{-1} (or 1.18 °C·hr hr^{-1}). Indeed, the climate-model fields downscaled via the Altostratus uWRF model suggest that the warming (relative to present conditions) increases in the NNE and NE directions in this region. This can also be seen in differences B1, B2, and B3 in Figure 6.

Graph C1 (in Figure 5) is a temporal comparison between absolute model fields at SAC in 2019 vs. TMY3. That is, the graph shows hour-to-hour comparisons between the model's absolute output for year 2019 versus TMY3 at SAC, hence the relatively large scatter. The model year 2019 shows a net warming (relative to TMY3) of 8722 °C·hr yr^{-1} (or almost 1.0 °C·hr hr^{-1} as an annual average – also see difference C1 in Figure 6) which has significant implications for current energy modeling and forecasting that still use outdated TMY data. The next two graphs are spatial comparison at AB (D1) and CTRS (D2), relative to SAC, all based on absolute meteorological model output for 2019. Thus this is a more dynamically-consistent set of data that can be inter-compared directly. In this case, AB sees a net warming of 5187 °C·hr yr^{-1} (or 0.59 °C·hr hr^{-1} over 8760 hours) relative to SAC, whereas as CTRS sees a net warming of 8149 °C·hr yr^{-1} (or 0.93 °C·hr hr^{-1}) relative to SAC (also see Figure 6, differences D1 and D2).

Finally, graphs E1, E2, and E3 (Figure 5) show a comparison of year 2050 vs. 2019 at each respective location (SAC, AB, and CTRS), all from model results (absolute fields, not perturbations). Thus, again, this is a dynamically-consistent set of variables that can be useful to compare. The differences at each location were already used above and mapped onto existing conditions to generate synthetic weather, as seen in graphs B1, B2, and B3 (Figure 5). Thus, these represent again local net warmings of 0.99 °C·hr hr^{-1}, 1.05 °C·hr hr^{-1}, and 1.18 °C·hr hr^{-1} at SAC, AB, and CTRS, respectively, as annual averages (over 8760 hours). The differences can also be seen in Figure 6 (E1, E2, and E3).

To wrap up this discussion, the absolute model fields for current climate (2019) and future year (2050 RCP 8.5) are compared with the TMY3 weather data for SAC. To do that, the last 6 datasets in Figure 6 are compared to TMY3 (the first dataset on the left in Figure 6).

Relative to TMY3 (at SAC), the 2019 all-hours average temperature at SAC is 0.99 °C higher – at AB it is 1.58 °C higher (than TMY3) and at CTRS it is 1.92 °C higher (than TMY3). The 2050 all-hours averaged temperature at SAC is 1.98 °C higher than TMY3, at AB it is 2.63 °C higher (than TMY3), and at CTRS, it is 3.10 °C higher (than TMY3). Since these are annual averaged differences (over 8760 hours), they are extremely significant.

Finally, it can also be stated that the intra-urban differences in temperature, caused by urban heat transport and local heat generation / urban surface properties, is of the same magnitude as the predicted local effects of climate change (in 2050, in this example). Spatially, in 2019, AB is warmer than SAC by an annual average of 0.59 °C and CTRS is warmer than SAC (in 2019) by an annual average of 0.93 °C (these spatial differences are based on model results). The changes in climate and land use produce a local warming of 1.05 °C at AB (in 2050 relative to 2019) and a warming of 1.18 °C at CTRS (in 2050 relative to 2019). Thus comparing 0.59 °C (spatial) to 1.05 °C (climate) and 0.93 °C (spatial) to 1.18 °C (climate) shows that the spatial impacts of intra-urban microclimate variations are of the same magnitudes as the local predicted impacts of climate change between now and 2050 (RCP 8.5).

Figure 7 summarizes the same type of analysis but for other meteorological variables. In this figure, rows R1 through R11 are defined as follows (y-axis vs. x-axis):

R1: AB vs. TMY3 (approach 1); **R2**: CTRS vs. TMY3 (approach 1); **R3**: SAC 2050 vs. TMY3 (approach 1); **R4**: AB 2050 vs. AB 2019 (approach 1); **R5**: CTRS 2050 vs. CTRS 2019 (approach 1); **R6**: SAC 2019 vs. TMY3 (approach 3); **R7**: AB 2019 vs. SAC 2019 (approach 3); **R8**: CTRS 2019 vs. SAC 2019 (approach 3); **R9**: SAC 2050 vs. SAC 2019 (approach 3); **R10**: AB 2050 vs. AB 2019 (approach 3); and **R11**: CTRS 2050 vs. CTRS 2019 (approach 3). The approaches were defined at the beginning of Section 2.

In Figure 7, DEW is in °C, DIFF, LW, and SW are in W m^{-2}, RH is in %, and WSP is in m s^{-1}.

[Figure 5 is on following page]

Figure 5: Comparisons of various temperature indicators (at SAC, AB, and CTRS)

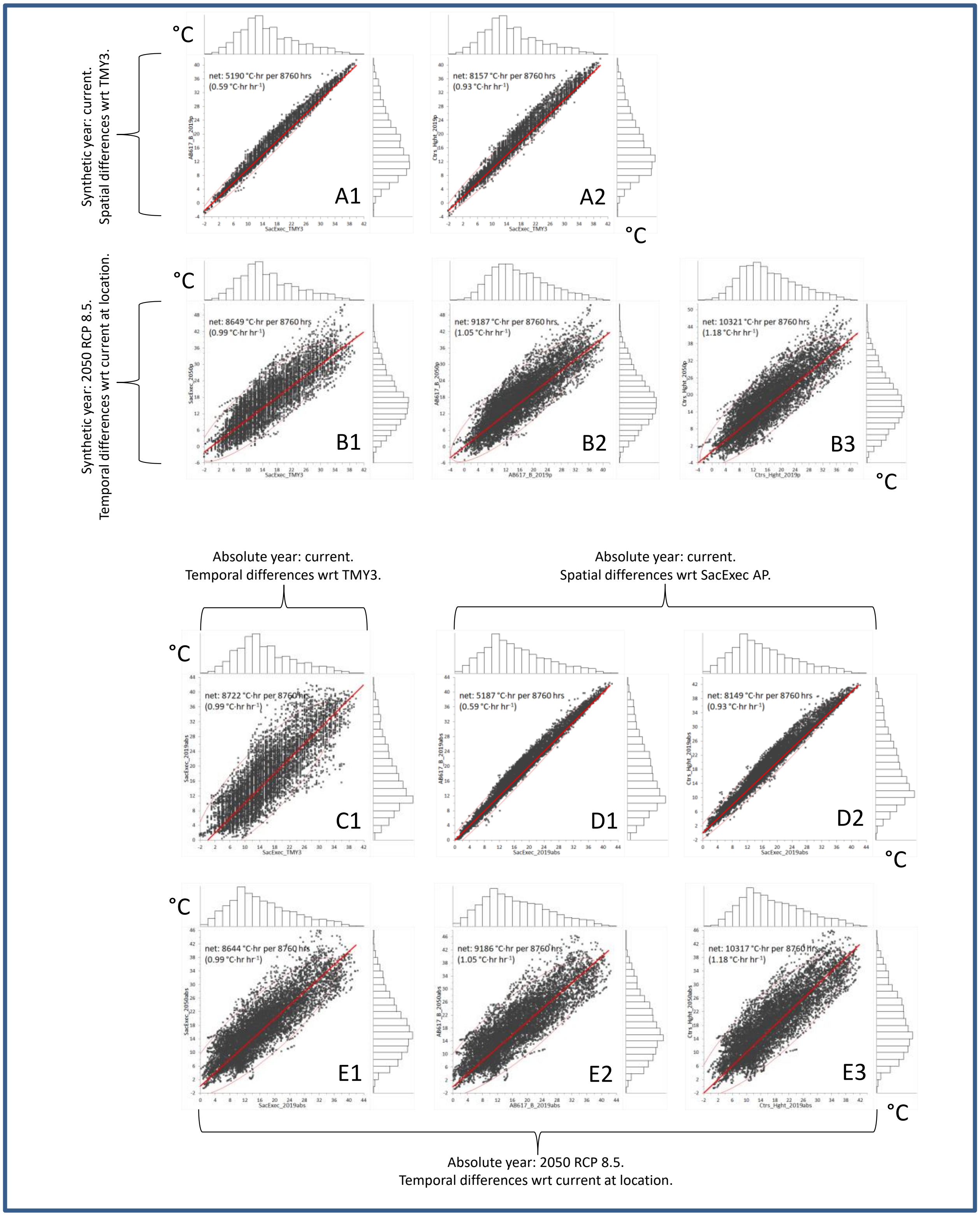

Figure 6: Descriptive statistics for 8760 hours of air temperature at SAC, AB, and CTRS.

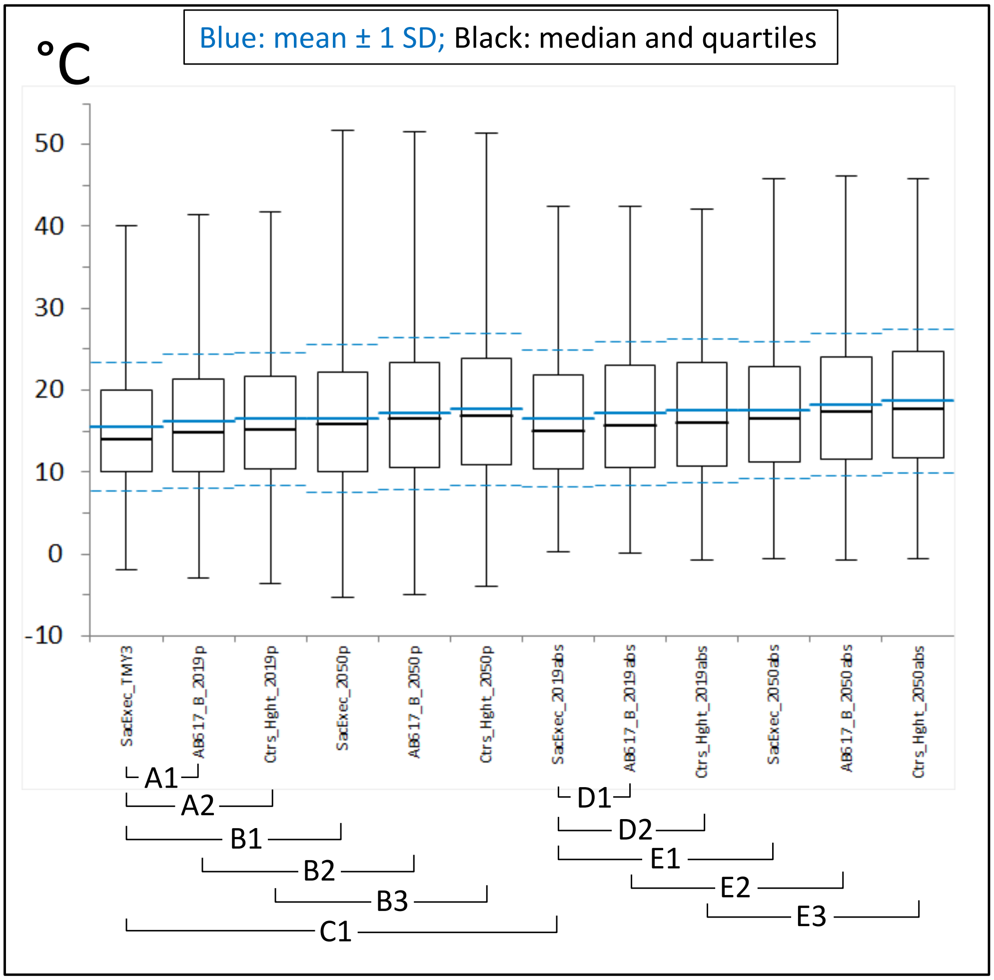

Note: At the bottom of the figure, differences are labeled for cross-referencing with graphs in Figure 5.

[Figure 7 is on following page]

Figure 7: Selected comparisons among variables.

(**DEW**: dew point; **DIFF**: diffuse radiation; **LW**: longwave radiation from sky; **RH**: relative humidity; **SW**: direct normal radiation; **WSP**: wind speed)